S-taper Fiber Based Moisture Sensing in Power Transformer Oil

Jun Jiang, *Senior Member, IEEE*, Ruihan Wu, Jinfeng Liu, Xuerui Wu, Qiang Wu, Prem Ranjan, Xiaoqin Zhang, Jun Liu

***Abstract*— A moisture sensing technique for real-time monitoring of the moisture content in transformer oil based on an S-taper fiber structure, is proposed and experimentally demonstrated, with the advantages of high sensitivity, excellent repeatability, simple fabrication, compact structure and resistance to ambient temperature variation. By analyzing the physical model of the S-taper fiber, the quantitative relationship between the wavelength change of the transmission dip in the transmission spectrum of the S-taper fiber and the moisture content is established. Then the S-taper fibers with different structural parameters, such as the waist diameter and the axial offset, were fabricated in the lab, and actual measurements in transformer oil samples with different moisture content are carried out. The results show that the transmission dip experiences a red-shifts with decreasing moisture, which could be used to correlate/trace moisture content. It is demonstrated that the S-taper fiber achieves higher detection sensitivity with a decreasing waist diameter or increasing axial offset. For the S-taper fiber with a waist diameter of 50 μm and an axial offset of 110 μm, the sensitivity and the lower detection limit reach up to 0.48 nm/ppm and 2.19 ppm, respectively. Therefore, the S-taper fiber sensor could effectively in-situ monitor the moisture content in the transformer oil in real-time, which helps to detect the insulation damp problem in the early stage of the transformer in time and ensure its long-term safe operation.**

***Index Terms* —Fiber sensor, Oil-immersed power transformer, Moisture content, Damp defect, Sensitivity**

I. INTRODUCTION

Oil-immersed transformer, one of the most vital equipment in a power system, undertakes the function of voltage transformation and energy transmission. The operational reliability of power transformer closely depends on its electrical insulation, which further determines the stability of the whole power system [1,2]. Especially, transformer oil plays a significant role in cooling and electrical insulation [3,4]. However, moisture is generated in the oil during the long-term operation and occurrence of electrical or thermal faults [5,6]. The increase in moisture content in oil inevitably reduces dielectric/insulation performance of the oil and accelerate the aging of oil/paper insulation system, which leads to the instability and potential threat [7]. Therefore, it is essential to detect and monitor the moisture content in transformer oil.

Numerous methods for the detection of moisture content in transformer oil have been reported, which can be classified into chemical [8,9], electrical [10-12], acoustic [13] and optical [14-26] techniques according to the corresponding working principles. Chemical chromatography and Karl-Fischer titration [8,9] are the most common moisture-in-oil detection methods in laboratory by virtue of their low detection limits and high precision. However, they are not suitable for online detection and oil sample contaminants might occur during the preparation of detection. Capacitive sensor, radio frequency (RF) technique and frequency domain spectroscopy (FDS) technique are applied as the electrical methods [10-12]. The key to these electrical methods is to find out the dielectric variance of the oil samples to calculate moisture content with the advantages of high sensitivity and low cost. Similarly, the ultrasonic method calculates the water content based on the principle that ultrasonic waves transmit at different speeds in various media [13]. However, the electrical and acoustic techniques suffer from cross-interference caused by electromagnetic radiation and environmental noise under actual working conditions.

Optical methods are widely studied because of their flexible layout, fast response, high sensitivity, resistance to electromagnetic interference and non-destructiveness. Among them, the near-infrared spectroscopy technique (NIRS) helps to determine the moisture content by combining specialized algorithms like partial least squares (PLS), genetic algorithms (GA), etc. under the characteristic wavelength of the absorption peaks of H_2O molecule [14,15]. Nevertheless, the low absorption coefficients, beam divergences, and free-space setup make NIRS not so accurate to detect gas or moisture. Instead, fiber-based optical approach is more practical. Fiber Bragg grating (FBG) sensors are usually coated with polyimide, poly methyl methacrylate (PMMA) or other moisture-absorbing materials to improve the performance of

Manuscript received Sep. xx, 2022; revised xxx, 2022; accepted xxxx, 202x. This work was supported in part by the National Natural Science Foundation of China (52177150), Project funded by China Postdoctoral Science Foundation (2022M720977), and Zhejiang Planned Projects for Postdoctoral Research Funds (ZJ2022114). (*corresponding author: Jun Jiang*)

Jun Jiang, Ruihan Wu, and Jinfeng Liu are with Jiangsu Key Laboratory of New Energy Generation and Power Conversion, Nanjing University of Aeronautics and Astronautics, Nanjing 211106, China.(e-mails: jiangjun0628@163.com; wran243255032@163.com; liujf0618@163.com).

Xuerui Wu is with the Research and Development Department, Alphapec Instrument, Yixin 443000, China. (m18437953200@163.com)

Qiang Wu is with the Faculty of Engineering and Environment, Northumbria University, Newcastle upon Tyne, U.K. Qiang Wu is also with the Key Laboratory of Nondestructive Test (Ministry of Education) of Nanchang Hangkong University, Nanchang, 330063, China (e-mail: qiang.wu@northumbria.ac.uk).

Xiaoqin Zhang is with State Grid Jiangsu Electric Power Co. Ltd. Research Institute, Nanjing 211103, China. (e-mail: 15850736276@126.com).

Prem Ranjan is with Deeside Centre for Innovation of National Grid UK, Deeside 6WHC+X2, United Kingdom (e-mail: ppremranjan@gmail.com).

Jun Liu is with Hangzhou Qianjiang Electric Group Co., Ltd, Hangzhou 311243, China. (e-mail: 929906286@qq.com)

moisture detection [16-18]. Nonetheless, FBG-based sensors are prone to be applied to relative humidity (RH) detection due to the sensitivity limitation, moreover, temperature cross-sensitivity always exists. Another fiber sensor based on evanescent-field was also proposed to detect moisture content with micro/nanofiber (MNF) [19] or cladding-less sapphire fiber helically wound by an electrode [20], but the probe fabrication is complicated.

In contrast, the S-taper fiber sensor is put forward owing to the advantages of high sensitivity, high repeatability, simple fabrication, compact structure and resistance to surrounding temperature change. At first, the S-taper fiber was used to detect surrounding refractive index (SRI), which determines the wavelength of the transmission dip of its transmission spectrum [21,22]. The refractive index induced wavelength shift has been validated to trace the physical quantity to be measured [23]. Furthermore, the S-taper fiber coated with polyvinyl alcohol [24], SiO_2 nanoparticles [25] and graphene oxide (GO) [26] is proposed, for the application of RH detection in air. Even the GO-coated S-taper fiber sensors were cascaded with FBG to achieve simultaneous detection of temperature and RH [27]. The key problem for those techniques is the non-stable measurement, particularly long-term stability due to the introduce of additional coating layer. However, the sensitivity should be improved compared to fiber sensor without coating RH sensitive layer. Moreover, the application of optical fiber sensor in transformer oil need to confront specific challenges, such as transmission loss, practical installation, cross-sensitivities, etc.

Motivated by the various benefits of the S-taper fiber, a fiber sensor to directly detect moisture content in transformer oil based on wavelength analysis is proposed in this paper. Firstly, the optical transmission characteristic and the sensing mechanism of a S-taper fiber are theoretically analyzed. Further, S-taper fiber probes with different structural parameters are prepared and the platform for moisture detection is built. Eight sets of oil samples with different moisture contents are prepared and used in moisture content detection tests. Finally, according to the experimental results, the effectiveness of this scheme for moisture detection is verified, and the structural parameters of S-taper fiber are optimized, to effectively improve the sensitivity of the S-taper fiber for sensing moisture. It shows the potential for the on-site determination of the moisture content in transformer oil.

II. Detection Principle of S-Taper Fiber Probe

S-taper fiber is a kind of microstructure fiber with "S" shape, which can be made by single-mode fiber (SMF), with the advantages of high repeatability, simple fabrication, compact size and high sensitivity. Due to its bending structure, the S-taper fiber produces inter-mode interference and is highly sensitive to refractive index (RI), so it is commonly applied to refractive index sensors [22].

The asymmetry bending structure of the S-taper fiber is shown in Fig. 1. There are three main structural parameters of the S-taper fiber: taper waist diameter (d_w), axial offset (L_{off}) and structural length (L_{all}). And λ represents incident light wavelength.

Due to the asymmetrical construction, it destroys the total reflection condition of the light within the S-taper fiber. When the incident light enters the first tapered region, a large proportion of the fundamental mode energy is coupled into the cladding from the core and propagates in the cladding in the form of higher order modes (also called the cladding modes). On the other hand, a small proportion of the fundamental mode energy continues to be transmitted in the core (also called the core mode). The core and cladding modes propagate through the sensing segment. During propagation to the second tapered region, the cladding modes are re-coupled back to the core and interfere with the core mode. A schematic diagram of light propagation in the S-taper fiber is shown in Fig. 1.

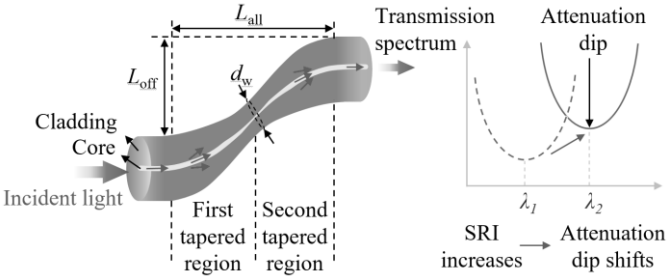

Fig. 1. Structural parameter and light transmission process in S-taper fiber

The transmitted light intensity of the S-taper fiber after inter-mode interference can be expressed as:

$$I = I_1 + I_2 + 2I_1 I_2 \cos\Delta\phi \tag{1}$$

Where, I_1 and I_2 denote the core mode intensity and the cladding mode intensity, respectively; and $\Delta\phi$ represents the phase difference between the core and cladding modes.

The phase difference between the cladding mode and the core mode can be calculated as:

$$\Delta\phi = \frac{2\pi\Delta n_{\text{eff}} L_{\text{eff}}}{\lambda} \tag{2}$$

Where, Δn_{eff} is the effective refractive index (ERI) difference between the ERIs of the core and the cladding modes, L_{eff} is the effective length of the S-tapered region.

When $\Delta\phi$ is equal to $(2k+1)\pi$, the transmission dip wavelength of the S-taper fiber transmission spectrum can be expressed as:

$$\lambda_m = \frac{2\Delta n_{\text{eff}} L_{\text{eff}}}{2m+1} \tag{3}$$

Where, m is the interference order.

The cladding modes are sensitive to the change in SRI, unlike the core mode [21]. Furthermore, Δn_{eff} is positive with the SRI increasing due to higher-order cladding modes, excited by the bending structure [22,28]. For the S-taper fiber applied to the detection of moisture content in transformer oil, the RI of the moisture-in-oil sample increases with the moisture content decreasing, leading to the increment of Δn_{eff}. According to Equation (3), the transmission dip wavelength of the S-taper fiber transmission spectrum would shift to longer wavelength. This red-shift varies with the moisture content,

thus the S-taper fiber can be used potentially for moisture detection in transformer oil. In addition, both Δn_{eff} and L_{eff} are affected by the structure parameters of S-taper fibers, such as the taper waist diameter and the axial offset. Hence the optimization of these two parameters is one of the effective ways to improve the detection sensitivity.

In order to study the quantitative relationship between moisture content in transformer oil and the wavelength shift of the transmission dip, and to investigate the effect of d_{w} and L_{off} on the detection sensitivity, it is necessary to carry out actual moisture detection based on the wavelength shift of the transmission dip as discussed in section 3.

III. Preparation of Oil Samples and S-taper Fiber Probes

Before conducting the experiments, transformer oil samples with different moisture contents were prepared, and S-taper fibers with different structural parameters were fabricated.

A. Preparation of moisture-in-oil samples

Eight moisture-in-oil samples were prepared by Karamay #25 transformer oil and pure water at room temperature. Different volumes of water were injected into the 100 mL transformer oil by 50 μL micro syringe. The RIs of the samples was measured by a 2WA-J Abbe refractometer. More detailed information of the oil sample is shown in Table 1. The analyzer (JWS-1) based on Karl-Fischer titration, with high detection limit and resolution, is used in our experiment. Hence the moisture detection performance of the S-taper fiber can be fully verified with the widely used reference.

TABLE I
Moisture Content and RIs of The Oil Samples

Sample	S1	S2	S3	S4
Moisture content (mg/L)	8.3	19.7	27.4	38.5
RI	1.4572	1.4571	1.4570	1.4568
Sample	S5	S6	S7	S8
Moisture content (mg/L)	49.6	60.8	78.9	89.2
RI	1.4567	1.4566	1.4564	1.4562

B. Fabrication of S-taper fiber probe

In this study, Corning 28 SMF with 9/125 μm was used to fabricate S-taper fiber by a special fusion splicer platform. The fabrication of the S-taper fiber involves four steps, as shown in Fig. 2.

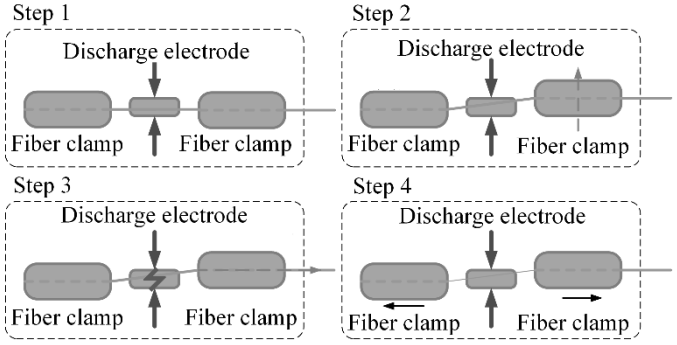

Fig. 2. Fabrication steps of S-taper fiber

In Step 1, the outer coating layer of the SMF was removed, then it was fixed on the fiber clamps to keep it straight without additional stress. In Step 2, the relative axial offset of the two fiber clamps was manually adjusted horizontally. During Step 3, the electrode was continuously discharged at a certain intensity for a period of time (1.4~2.2s), leaving SMF in a molten state. Step 4, fiber clamps were moving in reverse by non-axial pull. Then a S-taper fiber was obtained, its waist diameter and axial offset can be controlled by adjusting the axial offset of fiber clamps, the discharge current and discharge time.

The S-taper fibers, with d_{w} from 35 to 50 μm and L_{off} from 50 to 110 μm, were fabricated for moisture detection. A glass micrometer and electron microscope with camera function are used to measure the waist diameter and axial offset. Figure 3 shows microscope image of the fabricated S-taper fibers.

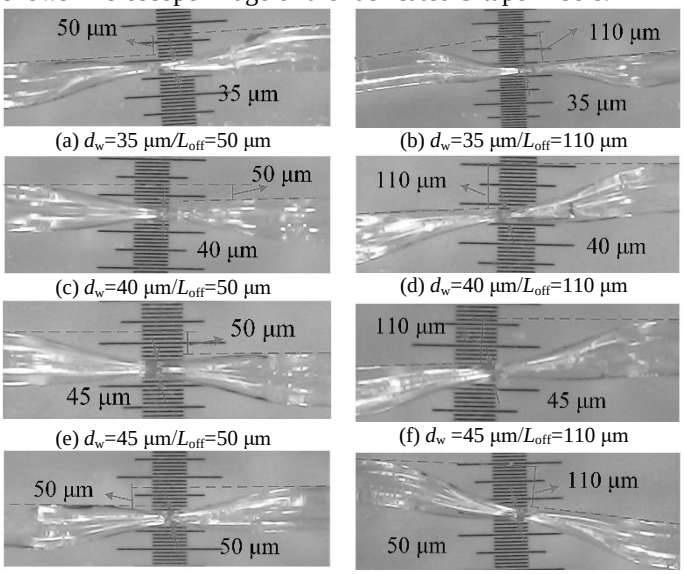

(a) d_{w}=35 μm/L_{off}=50 μm (b) d_{w}=35 μm/L_{off}=110 μm
(c) d_{w}=40 μm/L_{off}=50 μm (d) d_{w}=40 μm/L_{off}=110 μm
(e) d_{w}=45 μm/L_{off}=50 μm (f) d_{w} =45 μm/L_{off}=110 μm
(g) d_{w}=50 μm/L_{off}=50 μm (h) d_{w}=50 μm/L_{off}=110 μm

Fig.3. Enlarged figures of S-taper fibers with different structural parameters

In order to test the repeatability of the fabrication of the S-taper fiber, 6 groups of S-taper fibers with d_{w}=35 μm/L_{off}=110 μm were fabricated, and their actual waist diameters and axial offsets were measured, as shown in Fig. 4. The average errors of the waist diameters and axial offsets are 0.23% and 0.12%, respectively. Therefore, there is a good reproducibility in the fabrication process of the S-taper fiber, which is prospective for the practical exploitation.

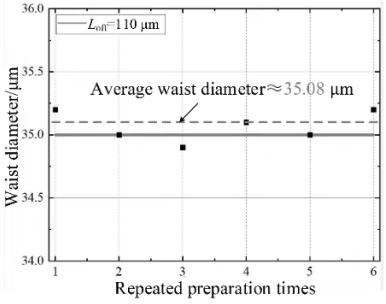

(a) The repeatability of the waist diameters of 35 μm

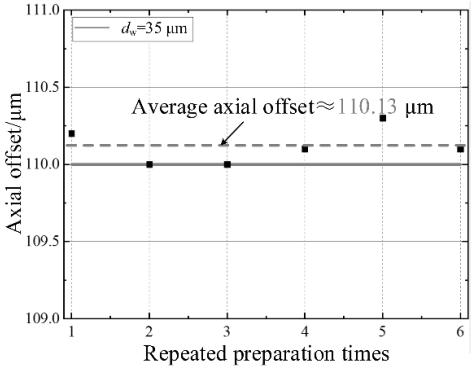

(b) The repeatability of the axial offsets of 110 μm

Fig. 4. The preparation repeatability of 6 S-taper fibers with d_w=35 μm/L_{off}=110 μm

IV. Experiments of Moisture Detection with S-taper Fiber

A. Experimental Setup for Moisture in Oil Detection

To detect moisture in the oil samples, the built experimental setup is shown in Fig. 5. All the experiments were conducted at room temperature in the lab. The light source is a broadband laser, Golight ASE, with the wavelength range of 1532~1564 nm and the intensity of 20 mW. The wavelength demodulation unit is used to detect the S-taper fiber transmission spectrum.

Especially, a compact oil chamber is designed to fill oils and install the S fiber probe.

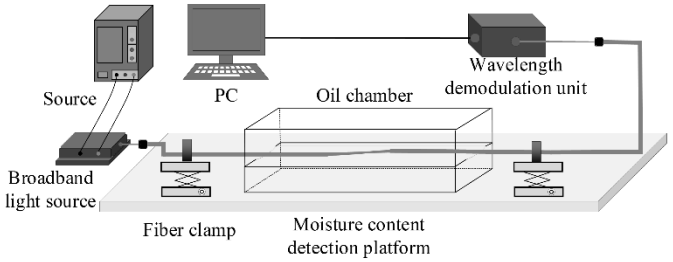

Fig. 5. The configuration of moisture-in-oil detection based on S-taper fiber

During the measurement of the moisture content in the oil samples, the S-taper fiber was fixed on a fiber holder to keep it straight. Then the sample was injected into the oil chamber until the S-taper fiber immediately immersed in the oil. After the transmission spectrum was recorded by the wavelength demodulation unit, the oil chamber was completely cleaned with ethanol. The procedure was repeated for each sample.

B. Effect of the axial offset on the detection sensitivity

To investigate the effect of the axial offset on the sensitivity of S-taper fibers, the S-taper fibers with the same waist diameter of 50 μm and the axial offsets of 50 μm/70 μm/90 μm/110 μm were fabricated by setting the discharge intensity and time.

In Fig. 6 (a), the transmission spectra of the S-taper fiber with d_w =50 μm/L_{off}=50 μm in different oil samples are plotted, in which the transmission dip experiences a red-shift with decreasing moisture, consistent with the detection principle of the S-taper fiber. The maximum red-shift of the transmission dip with the moisture content from 8.3 to 89.2 ppm is about 3.12 nm. In order to observe the wavelength red-shift of the sensors with L_{off}=70 μm/90 μm/110 μm more intuitively, only four spectral lines with large wavelength intervals are shown in Fig. 6 (b) (c) (d).

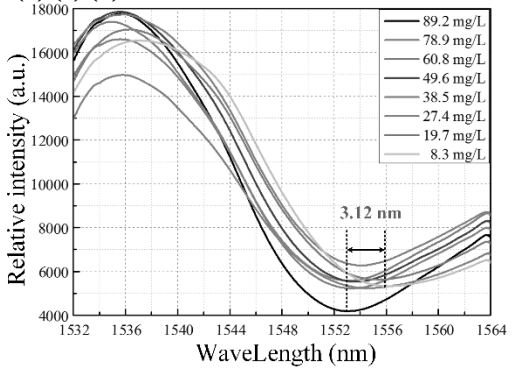

(a) d_w=50 μm/L_{off}=50 μm

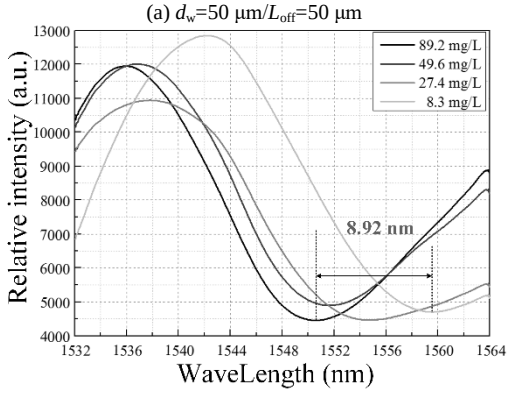

(b) d_w=50 μm/L_{off}=70 μm

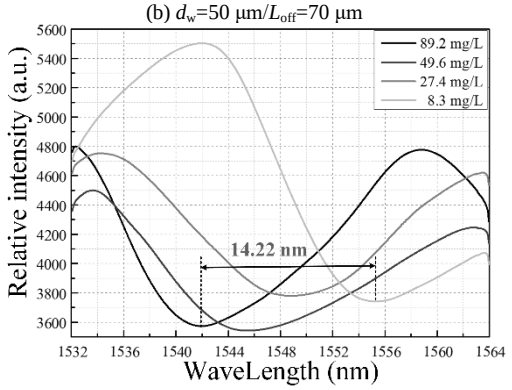

(c) d_w=50 μm/L_{off}=90 μm

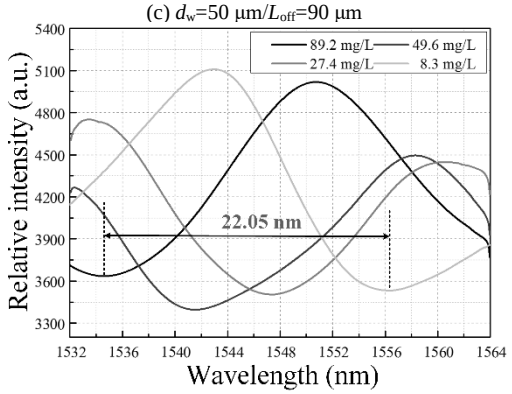

(d) d_w=50 μm/L_{off}=110 μm

Fig. 6. Transmission spectra when the S-taper fibers with different waist diameters are immersed into the samples.

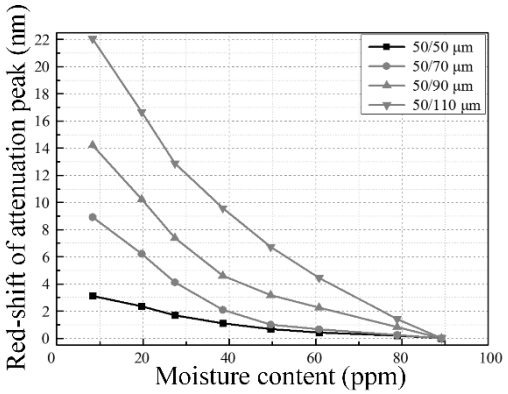

Fig. 7. The red-shift versus varying moisture content for S-taper fibers (the waist diameter of 50 μm) with different axial offsets

Fig. 7 illustrates the red-shifts of the transmission dip as a function of the moisture content for S-taper fiber with different axial offset. For the four curves, it can be found that the wavelength shift tends to increase with the decreasing moisture content. The curve of the S-taper fiber with L_{off}=110 μm is entirely above that with L_{off}=50 μm/70 μm/90 μm, which illustrates that the probe with a larger axial offset is more sensitive.

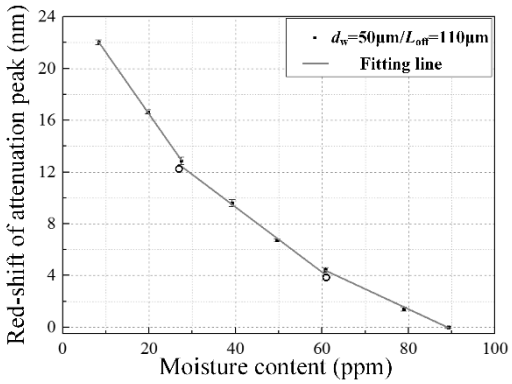

Fig. 8. The fitting curve of red-shift of the transmission dip in the three sensing regions for the S-taper fiber with d_w=50μm/L_{off}=110μm

After optimizing the axial offset, the S-taper fiber with d_w=50 μm/L_{off}=110 μm is used to investigate the relationship between the red-shift of the transmission dip and the moisture content. As shown in Fig. 8, there is an overall linear trend between the red-shift and the moisture content due to the variation of SRI, and error bars represent the distribution of 3 tests at each concentration. In order to improve the fitting performance and detection accuracy, the fitting area can be classified into three linear sections. In the moisture content range of 8.3~27.4 ppm, 27.4~60.8 ppm, and 60.8~89.2 ppm, the corresponding average sensitivities are 0.48 nm/ppm, 0.25 nm/ppm and 0.16 nm/ppm. The sensitivity of the S-taper fiber with d_w =50 μm/L_{off}=110 μm reaches 0.48 nm/ppm, the highest sensitivity in the range of 8.3 ppm~27.4 ppm.

C. Effect of the waist diameter on the detection sensitivity

The waist diameter is also a key parameter in determining the sensitivity of the S-taper fiber like the axial offset. In order to investigate the effect of the waist diameter on S-taper fiber, the S-taper fibers with the same axial offset of 90 μm and the waist diameter of 35 μm/40 μm/45 μm/50 μm were tested.

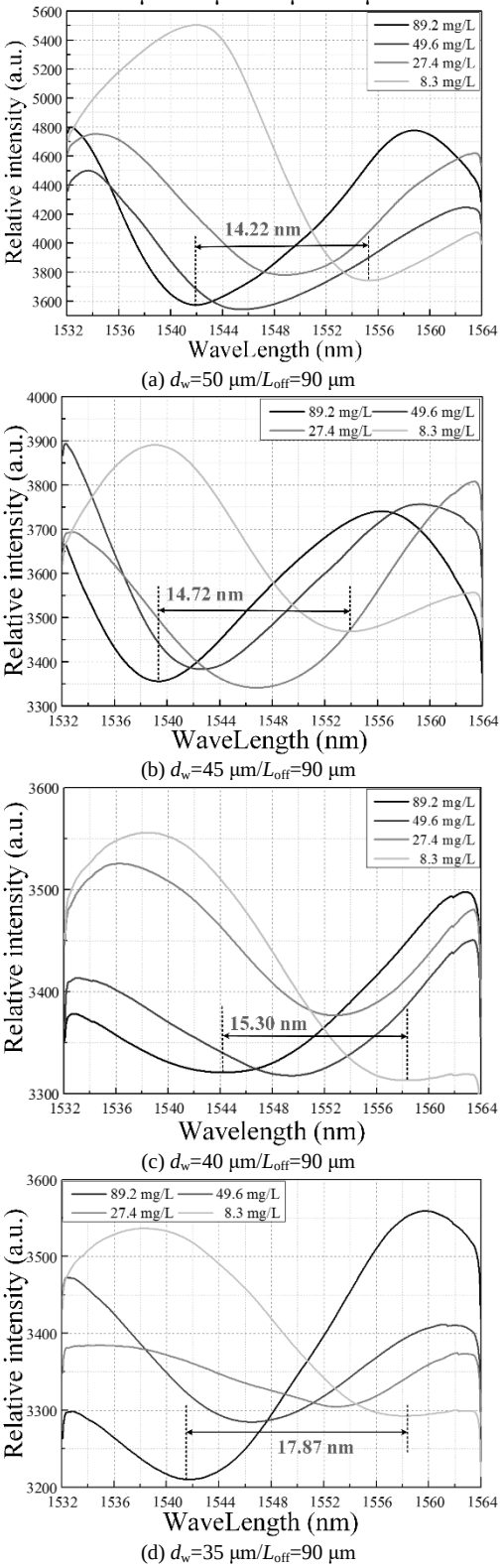

Fig. 9. Transmission spectra when the S-taper fibers with different waist diameters are immersed into the samples.

The curves in Fig. 9 represent cases of the S-taper fiber with d_w=35 μm/40 μm/45 μm/50 μm in different moisture concentrations of oil sample, which also shows that the transmission dip experiences a red-shift with the moisture decreasing, and a smaller waist diameter leads to a larger

wavelength shift of the transmission dip.

As shown in Fig. 10, for the S-taper fiber with d_w=35 μm/40 μm/45 μm/50 μm, the transmission dip shifts to shorter wavelength monotonically with the increase of the moisture content. In particular, the S-taper fiber with d_w=35 μm with the higher slope is more sensitive than that with d_w=40 μm/45 μm/50 μm.

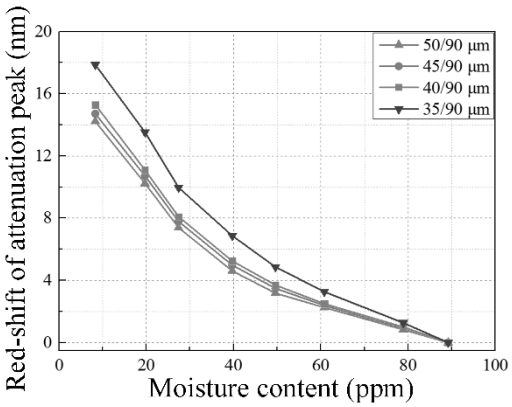

Fig. 10. The red-shift versus varying moisture content for S-taper fibers (the axial offset of 90μm) with different waist diameters

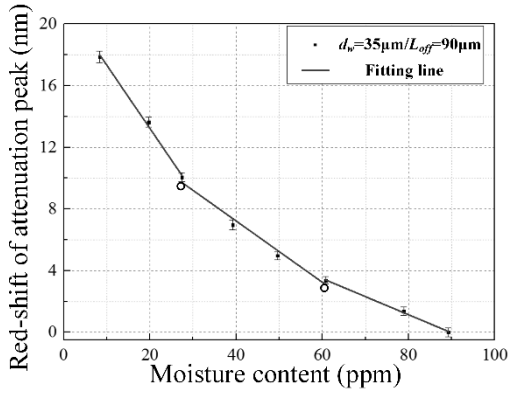

Fig. 11. The fitting curve of red-shift of the transmission dip in the three sensing regions for the S-taper fiber with d_w=35 μm/L_{off}=90 μm

After optimizing the waist diameter, the S-taper fiber with d_w=35 μm/L_{off}=90 μm is selected to investigate the relationship between the redshift of the transmission dip and the moisture content, which is shown in Fig. 11. Error bars represent the distribution of 3 tests at each concentration. The average sensitivities in the moisture content range of 8.3~27.4 ppm, 27.4~60.8 ppm and 60.8~89.2 ppm by linear fitting is 0.41 nm/ppm, 0.20 nm/ppm and 0.21 nm/ppm, respectively.

D. Comprehensive effect of the waist diameter and axial offset

It should be noted that the impact of the waist diameter and axial offset is interactional during the fabrication of the S-taper fiber sensor. Additionally, the actual range of waist diameter and axial offset is different, the relative change of the values needs to considered at the same time. To investigate the comprehensive effect of waist diameter and axial offset on moisture detection, the S-taper fibers with d_w=35~50 μm (a step of 5 μm) and L_{off}=50~110 μm (a step of 20 μm) were fabricated. The maximum red-shifts of the transmission dip in the moisture content range from 8.3 to 89.2 ppm were recorded, in Table 2, to characterize the detection sensitivity of the S-taper fibers with different structural parameters. However, it was found during the experiment that the transmission dip was undetected when the S-taper fibers with d_w=35~45 μm and L_{off}=110 μm were immersed in the oil sample with the low moisture content of 8.3 ppm. Herein, modes energy and inter-mode interference were critically weakened as the ERI of the cladding modes was close to the oil sample. As a consequence, the transmission dip became smaller and even disappeared, resulting in missing data in Table 2.

It can be inferred that the boundary of the waist should be larger than 45 μm within the predefined axial offset of 110 μm in order to avoid excessive light attenuation.

TABLE II
THE MAXIMUM RED-SHIFTS OF THE TRANSMISSION DIP OF THE S-TAPER FIBER WITH DIFFERENT STRUCTURAL PARAMETERS

The maximum red-shifts of the transmission dip (nm)				
d_w \ L_{off}	50 μm	70 μm	90 μm	110 μm
50 μm	3.12	8.92	14.22	22.05
45 μm	3.95	10.18	14.72	/
40 μm	4.38	10.94	15.30	/
35 μm	7.07	12.80	17.87	/

From Table 2, without considering the S-taper fiber with L_{off}=110 μm, it can be seen that the maximum red-shift increases as the waist diameter decreases or the axial offset increases. As for the S-taper fiber with d_w=35~45 μm and L_{off}=110 μm, its maximum red-shift was still in line with this trend.

It can be seen that the S-taper fiber with d_w=50 μm and L_{off}=110 μm shows the largest maximum red-shift of 22.05 nm and its moisture detection range is larger than with d_w=35~45 μm and L_{off}=110 μm. Therefore, d_w=50 μm and L_{off}=110 μm are the optimal structural parameters optimization of S-taper fibers to enhance the detection sensitivity. Its average sensitivities in the moisture content ranging from 8.3 ppm to 27.4 ppm is 0.48 nm/ppm. The average wavelength fluctuation caused by noise from the ASE laser data acquisition equipment and environment is about ±0.35 nm, accordingly the lower limit of moisture detection is calculated as 2.19 ppm, where 3 times of maximum wavelength variation (3 × 0.35 = 1.05 nm) is defined as measurement limit.

According to IEC 60422-2013 [29], for mineral insulating oil after filling in new electrical equipment prior to energization above 72.5 kV, the recommended moisture limit is 10 ppm. And as for mineral insulating oil in normal condition, in operating electrical equipment, the recommended moisture limit to take a remedial action is 15 ppm. By comparison, the lower limit of moisture detection of 2.19 ppm is much lower than that of the two recommended moisture limits. On the other hand, cross-sensitivity of temperature is slight owing to the offset and compromise between thermo-optical effect and thermal expansion in S-taper fiber. In addition, the dissolved gases contribute nothing to the refractive index [30]. Therefore, the S-taper with d_w=50 μm

and L_{off}=110 μm sufficiently meets the actual online monitoring needs of oil-immersed power transformers in operation.

V. Conclusion

In order to improve the ability of detecting moisture in transformer oil, an optical sensing scheme based on S-taper fiber with compact structure, fabrication simplicity, high sensitivity is proposed in this paper. The sensing principle, fabrication process and parameters optimization and sensing test of S-taper fiber are explored. The following conclusions can be obtained:

1) S-taper fiber, in which the core mode interferes with the cladding mode, is sensitive to the change of SRI. The dip of the transmission spectrum of the S-taper fiber experiences a red-shift with the decreasing moisture content. Therefore, the moisture content in oil can be obtained by measuring the wavelength shift of the S-taper probe.

2) The experimental results show that the sensitivity of S-taper fiber could be improved by increasing the axial offset and decreasing the taper waist diameter meanwhile considering the light intensity attenuation. Therefore, it is a feasible method to optimize moisture detection in oils by increasing the axial offset and decreasing the taper waist diameter of the S-taper fibers.

3) The S-taper fiber with d_w=50 μm and L_{off}=110 μm is the highest sensitive among all test S-taper fibers, and its sensitivity can reach up to 0.48 nm/ppm in the moisture content range of 8.3~27.4 ppm. Its detection lower limit is 2.19 ppm which meets the requirement of moisture detection in oil-immersed power transformers.

References

[1] V. Vasovic, et al., "Aging of transformer insulation — experimental transformers and laboratory models with different moisture contents: Part I — DP and furans aging profiles," *IEEE Trans. Dielectr. Electr. Insul.*, vol. 26, no. 6, pp. 1840-1846, Dec. 2019.

[2] D. Yang, W. Chen, F. Wan, Y, et al., "Identification of the Aging Stage of Transformer Oil-Paper Insulation via Raman Spectroscopic Characteristics," *IEEE Trans. Dielectr. Electr. Insul.*, vol. 27, no. 6, pp. 1770-1777, Dec. 2020.

[3] J. Jeong, J. An and C. Huh, et al., "Accelerated aging effects of mineral and vegetable transformer oils on medium voltage power transformers," *IEEE Trans. Dielectr. Electr. Insul.*, vol. 19, no. 1, pp. 156-161, Feb. 2012.

[4] M. Rajnak et al., "Transformer oil-based magnetic nanofluid with high dielectric losses tested for cooling of a model transformer," *IEEE Trans. Dielectr. Electr. Insul.*, vol. 26, no. 4, pp. 1343-1349, Aug. 2019.

[5] P. Przybylek, et al., "The influence of temperature and aging of cellulose on water distribution in oil-paper insulation," *IEEE Trans. Dielectr. Electr. Insul.*, vol. 20, no. 2, pp. 552-556, Apr. 2013.

[6] B. Garcia, J. C. Burgos, A. M. Alonso, et al., "A moisture-in-oil model for power transformer monitoring - Part I: Theoretical foundation," *IEEE Trans. Power Del.*, vol. 20, no. 2, pp. 1417-1422, Apr. 2005.

[7] J. P. Jiang, B. X. Du and A. Cavallini, "Effect of moisture migration on surface discharge on oil-pressboard of power transformers under cooling," *IEEE Trans. Dielectr. Electr. Insul.*, vol. 27, no. 5, pp. 1743-1751, Oct. 2020.

[8] J. Jalbert, R. Gilbert, and P. Tétreault, "Simultaneous Determination of Dissolved Gases and Moisture in Mineral Insulating Oils by Static Headspace Gas Chromatography with Helium Photoionization Pulsed Discharge Detection," *Anal. Chem.*, vol. 73, no. 14, pp. 3382-3391, Jul. 2001.

[9] A. Cedergren, S. Jonsson, "Progress in Karl Fischer Coulometry Using Diaphragm-Free Cells," *Anal. Chem.*, vol. 73, no. 22, pp. 5611-5615, Nov. 2001.

[10] Aslam, M. Zubair, and T. B. Tang, "A High Resolution Capacitive Sensing System for the Measurement of Water Content in Crude Oil," *Sensors*, vol. 14, no. 7, pp. 11351-11361, Jun. 2014.

[11] Z. X. Chen, W. F. Wu, et al. "Design and Analysis of a Radio-Frequency Moisture Sensor for Grain Based on the Difference Method," *Micromachines*, vol. 12, no. 6, pp. 708, Jun. 2021.

[12] Q. Xu, S. Wang, F. Lin, et al., "Moisture Assessment of Oil-Immersed Paper Based on Dynamic Characteristics of Frequency Domain Spectroscopy," *IEEE Access*, vol. 10, pp. 15183-15192, Feb. 2022.

[13] G. Andria, F. Attivissimo, A. D. Nisio, et al., "Design of a microwave sensor for measurement of water in fuel contamination," *Meas.*, vol. 136, pp. 74-81, Dec. 2019.

[14] D. Cassanelli, N. Lenzini, L. Ferrari, et al., "Partial Least Squares Estimation of Crop Moisture and Density by Near-Infrared Spectroscopy," *IEEE Trans. Instrum. Meas.*, vol. 70, pp. 1-10, Jan. 2021.

[15] T. A. Lestander, R. Leardi, "Selection of near Infrared Wavelengths Using Genetic Algorithms for the Determination of Seed Moisture Content," *Near Infrared Spectrosc*, vol. 11, no. 6, pp. 433-446, Nov. 2003.

[16] J. Jiang, X. Wu, Z. Wang, et al. "Moisture Content Measurement in Transformer Oil Using Micro-nano Fiber," *IEEE Trans. Dielectr. Electr. Insul.*, vol. 27, no. 6, pp. 1829-1836, Dec. 2020.

[17] W. Zhang and D. J. Webb. "PMMA Based Optical Fiber Bragg Grating for Measuring Moisture in Transformer Oil," *IEEE Photonics Technol. Lett.*, vol. 28, no. 21, pp. 2427-2430, Nov. 2016.

[18] L. S. M. Alwis, H. Bustamante. "Evaluation of the durability and performance of FBG-based Sensors for monitoring moisture in an aggressive gaseous waste sewer environment," *J. Lightwave Technol.*, vol. 35, no. 16, pp. 3380-3386, Aug. 2017.

[19] T. L. Yeo, Tong Sun, K. T. V. Grattan. "Polymer-coated fiber Bragg grating for relative humidity sensing," *IEEE Sens. J.*, vol. 5, no. 5, pp. 1082-1089, Oct. 2005.

[20] M. Holzki, H. Fouckhardt. "Evanescent-field fiber sensor for the water content in lubricating oils with sensitivity increase by dielectrophoresis," *Sens. Actuators, A*, vol. 184, pp. 93-97, Jul. 2012.

[21] R. Yang, Y. S. Yu, Y. Xue, et al. "Single S-tapered fiber Mach–Zehnder interferometers," *Opt. Lett.*, vol. 36, no. 23, pp. 4482-4484, Dec. 2011.

[22] M.L. Yang, Y. Yao. H, Zhang, et al. "In-line microfluidic sensor based on dual S-taper fiber interferometer for measurement of glucose concentration," *Optical Engineering*, vol. 61, no. 7, pp. 07101, Jul. 2022.

[23] Gong T., Liu X., Wang Z., et al. A highly sensitivity humidity sensor based on mismatching fused fiber Mach–Zehnder interferometric without moisture material coating. *Journal of Optics*, vol. 22, no. 2, pp. 025801, Jan. 2020.

[24] H. F. Liu, H. Zhang, B. Liu, et al. "Relative humidity sensor based on S-tapered fiber coated with polyvinyl alcohol," *Asia Communications and Photonics Conference 2014*, pp. ATh3A.199, Nov. 2014.

[25] H. F. Liu, Y. P. Miao, B. Liu, et al. "Relative Humidity Sensor Based on S-Taper Fiber Coated with SiO_2 Nanoparticles," *IEEE Sens. J.*, vol. 15, no. 6, pp. 3424-3428, Jun. 2015.

[26] Y. Zhao, A. W. Li, Q. Guo, et al. "Relative humidity sensor of S fiber taper based on graphene oxide film," *Opt. Commun.*, vol. 450, pp. 147-154, May 2019.

[27] Z. Lv, P. Niu, J. Jiang, et al. "Reflective SFT-FBG Hybrid Micro-Probe for Simultaneous Measurement of Relative Humidity and Temperature," *IEEE Photonics J.*, vol. 14, no. 1, pp. 1-6, Feb. 2022.

[28] C. Chen, R. Yang, et al. "Compact refractive index sensor based on an S-tapered fiber probe," *Opt. Mater. Express*, vol. 8, no. 4, pp. 919-925, Apr. 2018.

[29] Mineral insulating oils in electrical equipment – Supervision and maintenance guidance, IEC 60422, International Electrotechnical Commission, Geneva, Switzerland, Jun 2013.

[30] D. K. Mahanta and S. Laskar. "Water Quantity-Based Quality Measurement of Transformer Oil Using Polymer Optical Fiber as Sensor," *IEEE Sens. J.*, vol. 18, no. 4, pp. 1506-1512, Feb. 2018.

Jun Jiang (S'15-M'16-SM'20) was born in Anqing, China, in 1988. He received the B. E. degree in electrical engineering and automation from China Agricultural University (CAU) in 2011 and Ph.D. degree in high voltage and electrical insulation from North China Electric Power University (NCEPU) in 2016. During 2019-2020, he joined High Voltage Engineering Division, Department of Electrical & Electronic Engineering, School of Engineering, The University of Manchester (UoM), UK as Honorary Staff/Academic Visitor. He is now working as an Associate Professor in Department of Electric Engineering, Nanjing University of Aeronautics and Astronautics (NUAA), Nanjing, China. His research interests are condition monitoring of power apparatus and optical sensing application.

Ruihan Wu was born in Yichun, Jiangxi, China, in 1998. He received the B.E. degree in Nanchang University (NCU), Jiangxi, China, in 2021. He is currently pursuing the master's degree with the Department of Electrical Engineering, Nanjing University of Aeronautics and Astronautics (NUAA), Nanjing, China. His research interests are condition monitoring of power apparatus and optical sensing application.

Jinfeng Liu was born in Liao'cheng, Shandong, China, in 2000. She received the B.E. degree in Qufu Normal University (QFNU), Shandong, China, in 2022. She is currently pursuing the master's degree with the Department of Electrical Engineering, Nanjing University of Aeronautics and Astronautics (NUAA), Nanjing, China. Her research interests are condition monitoring of power apparatus, especially in the field of bushings.

Xuerui Wu was born in Xinyang, Henan, China, in 1995. He received the B.E. degree in electrical engineering from Henan University of Science and Technology (HAUST), Luoyang, China, in 2018. She received the Master degree in Department of Electric Engineering, Nanjing University of Aeronautics and Astronautics (NUAA), Nanjing, China in 2022. Currently she is working in Alphapec Instrument Co. Her research interests are advanced sensing applications.

Qiang Wu received the B.S. and Ph.D. degrees from Beijing Normal University and Beijing University of Posts and Telecommunications, Beijing, China, in 1996 and 2004, respectively. From 2004 to 2006, he worked as a Senior Research Associate in City University of Hong Kong. From 2006 to 2008, he took up a research associate post in Heriot-Watt University, Edinburgh, U.K. From 2008 to 2014, he worked as a Stokes Lecturer at Photonics Research Centre, Dublin Institute of Technology, Ireland. He is an Associate Professor / Reader with Faculty of Engineering and Environment, Northumbria University, Newcastle Upon Tyne, United Kingdom. His research interests include optical fiber interferometers for novel fiber optical couplers and sensors, nanofiber, microsphere sensors for bio-chemical sensing, the design and fabrication of fiber Bragg grating devices and their applications for sensing, nonlinear fibre optics, surface plasmon resonant and surface acoustic wave sensors.

Prem Ranjan (S'19, M'20) obtained the B.Tech. degree in Electrical and Electronics Engineering from NIT Calicut in 2015 and the MS, PhD degrees in Electrical Engineering from IIT Madras, India in 2019. He worked as a postdoc researcher at High Voltage Lab, The University of Manchester, UK till 2022. Currently, he is working as a test enginner at Deeside Centre for Innovation of National Grid UK. His current research interests include exploding wire and condition monitoring of power apparatus.

Xiaoqin Zhang was born in Nantong, Jiangsu, China, in 1989. She received the M.A. degree in Nanjing University (NJU), Jiangsu, China, in 2014. She is currently working in the State Grid Jiangsu Electric Power Co., Ltd. Research Institute, Nanjing, China. Her research interests are condition monitoring and fault diagnosis of power apparatus.

Jun Liu was born in Urumqi, Xinjiang, China, in 1973. He received the B.E. degree in Xinjiang University, China, in 1995. He is currently working the Research department of Hangzhou Qiantang River Electric Group Co., Ltd, Hangzhou, China. His research interests are condition monitoring of power transformer.